

Article

## Immunosensor Incorporating Anti-His (C-term) IgG F(ab') Fragments Attached to Gold Nanorods for Detection of His-Tagged Proteins in Culture Medium

Michał Wąsowicz <sup>1</sup>, Małgorzata Milner <sup>2</sup>, Dorota Radecka <sup>2</sup>, Krystyna Grzelak <sup>2</sup> and Hanna Radecka <sup>1,\*</sup>

<sup>1</sup> Institute of Animal Reproduction and Food Research, Polish Academy of Sciences, Tuwima 10, 10-747 Olsztyn, Poland; E-Mail: m.wasowicz@pan.olsztyn.pl

<sup>2</sup> Institute of Biochemistry and Biophysics, Polish Academy of Sciences, Pawińskiego 5a, 02-106 Warsaw, Poland; E-Mails: gosiam@ibb.waw.pl (M.M.); dorota.radecka@student.uw.edu.pl (D.R.); kg@ibb.waw.pl (K.G.)

\* Author to whom correspondence should be addressed; E-Mail: hanna.radecka@pan.olsztyn.pl; Tel.: +48-89-523-4636; Fax: +48-89-524-0124.

Received: 1 April 2010; in revised form: 13 May 2010 / Accepted: 20 May 2010 /

Published: 1 June 2010

---

**Abstract:** Immunosensors based on gold electrodes (electrochemical) or gold discs (optical) modified with 1,6-hexanedithiol, gold nanorods and Anti-His (C-term) monoclonal antibody F(ab') fragment are described. The antigen detected by the sensing platform is a recombinant histidine-tagged silk proteinase inhibitor (rSPI2-His<sub>6</sub>). Electrochemical impedance spectroscopy (EIS) and surface plasmon resonance (SPR) techniques were used as methods for detection of the antigen. This approach allows to detect the antigen protein in concentration of 10 pg per mL (0.13 pM) of culture medium. The immunosensor shows good reproducibility due to covalent immobilization of F(ab') fragments to gold nanorods layer.

**Keywords:** His-tag; F(ab'); gold electrodes; nanorods

---

## 1. Introduction

Histidine-tagged recombinant proteins are widely used in industry and research. The *Pichia* system allowing the production of heterologous proteins is among the most popular [1-3]. Most often a polyhistidine-tag consists of six histidine residues at the C- or N-terminus of the proteins (His<sub>6</sub>-tag). It facilitates the detection and purification of proteins. The tag is poorly immunogenic and generally does not affect the secretion, compartmentalization or folding of the fusion protein within the cell. In most instances, the His-tag does not interfere with the function of proteins as demonstrated for a wide variety of proteins, including enzymes, transcription factors and vaccines [4,5]. Developing a fast, easy and cost-effective detection method of His-tagged proteins would allow for efficient screening of biotechnological processes of proteins production. Currently protein assay relies mostly on popular immunodetection systems including ELISA and Western blot techniques [6]. These are relatively time-consuming and require costly reagents compared to biosensor approach. Immunosensors are a promising alternative to currently used detection systems [7-10]. They are analytical devices comprised of antibodies or their fragments coupled to a transducer and able to generate analytical response related to analyte concentration in a sample. Their ease of use and no need for expensive reagents required for the assay make them an optimal detection system for many purposes [11-14].

Improving immunosensor longevity and selectivity in complex matrices is still a subject of ongoing research. One of the most crucial issues of immunosensor fabrication is associated with the loss of biological activity upon immobilization of antibodies, because of their random orientation on support surfaces [7-10].

In general, the immunoglobulin molecule consists of two polypeptide chains F(ab')<sub>2</sub> responsible for antigen binding, and an Fc domain, which is not involved in these interaction. The Fc could be removed by enzyme digestions [15,16]. The prepared F(ab')<sub>2</sub> or F(ab') fragments could be self assembled on the gold surface or other functionalized supports due to disulfide or thiol group from the hinge region of immunoglobulin G [17-22].

The immunosensor fabrication process proposed here is shown in Scheme S1 (Supporting Information). The gold nanorods (GNR) have been applied for the underlayer of the immunosensor because of their excellent electron conductivity (EIS measurements) and optical properties (SPR measurements). Gold nanorods are interesting for use in biosensor fabrication thanks to their more suitable properties compared to spherical nanoparticles such as gold colloid.

The end facets of anisotropic Au nanorods are dominated by {111} planes and the side facets by {100} and {110} planes. It was reported that thiol derivatives preferentially bind to the {111} planes of Au nanorods [23-25]. This specific interactions allow Au nanorods assembly perpendicular towards the gold support with using dithiols as the linkers. In contrast, assembling of spherical isotropic Au nanoparticles create ordered 2-D and 3D structures, which are less suitable for selective binding of molecules on the surface [23-25]. The assembling of GNRs onto dithiol SAM deposited on the Au support create well ordered conductive layer with {111} planes on the surface, which is very suitable for oriented covalent immobilization of receptor through Au-S bonding. So, utilizing GNRs in biosensor designing is more efficient compare to using nanoparticles with spherical structures [26].

The study presented concerns the selective binding of antigen rSPI2-His<sub>6</sub> present in the sample solution by F(ab') fragment of antibody immobilized on a surface of the electrode was observed using electrochemical impedance spectroscopy (EIS) as well as surface plasmon resonance (SPR).

## 2. Experimental Section

### 2.1. Chemicals

Alumina 0.3 and 0.05  $\mu\text{m}$  was purchased from Buehler (USA). 1,6-Hexanedithiol (1,6-HDT), L-glycine (Gly), sodium azide ( $\text{NaN}_3$ ), potassium ferro- and ferricyanides, cetyltrimethylammonium bromide, tetraoctylammonium bromide, gold (III) chloride ( $\text{HAuCl}_4$ ), and PBS buffer components ( $\text{NaCl}$ ,  $\text{KCl}$ ,  $\text{Na}_2\text{HPO}_4$ ,  $\text{KH}_2\text{PO}_4$ ) were purchased from Sigma-Aldrich (Germany). Sulphuric acid, hydrochloric acid, silver nitrate, ethanol, cyclohexane, acetone, and methanol were purchased from POCh (Poland). Anti-His (C-term) monoclonal antibody and bovine serum albumin (BSA) was purchased from Invitrogen Life Technologies (Germany). All aqueous solutions were prepared using deionised water, resistivity 18.2  $\text{M}\Omega\text{cm}$  (Millipore). Reagents and solvents were of analytical purity and used without any purification steps. Experiments were carried out at room temperature unless stated otherwise.

### 2.2. Preparation of F(ab') fragments

According to the manufacturer's instructions a portion of papain agarose from papaya latex (Sigma) was suspended in 400  $\mu\text{L}$  of  $\text{H}_2\text{O}$  and incubated at 4  $^\circ\text{C}$  for 2 hours, stirring every 15 minutes. Subsequently, the suspension was centrifuged for 5 min (20  $^\circ\text{C}$ , 600 g). Then the papain agarose was rinsed twice in the activation buffer (50 mM  $\text{Na}_2\text{HPO}_4$ , 20 mM L-cysteine, 1 mM EDTA, pH 7) and activated in the same buffer at 37  $^\circ\text{C}$  for 20 min with shaking. Further the papain agarose was washed three times with 3 x digestion buffer (150 mM  $\text{Na}_2\text{HPO}_4$ , 3 mM EDTA, pH 7.0), and suspended in 2 x digesting buffer (100 mM  $\text{Na}_2\text{HPO}_4$ , 2 mM EDTA, pH 7.0) to the final concentration of 1  $\mu\text{g}/\mu\text{L}$ . This pre-activated papain agarose was used to prepare F(ab') fragments from Anti-His(C-term) antibody (Invitrogen). IgG (6  $\mu\text{g}$ ) was digested in 1x digestion buffer (50 mM  $\text{Na}_2\text{HPO}_4$ , 1 mM EDTA, pH 7.0; 20  $\mu\text{L}$ ) at 37  $^\circ\text{C}$  for 1 hour with constant shaking. The ratio of papain agarose to IgG was about 1:2 (w/w). The digestion was finished by centrifugation (5 minutes, 4  $^\circ\text{C}$ , 1,000 g) and the supernatant was used for polyacrylamide gel analysis (Figure S1) and preparation of immunosensor.

### 2.3. Preparation of antigens (rSPI2 proteins)

SPI2 cDNA was cloned into the pPICZ $\alpha$ B plasmid carrying the sequences encoding of myc epitope and polyhistidine tag. Transformation of *Pichia pastoris* cells (SMD 1168) by the pPICZ $\alpha$ B/SPI2 plasmid and the production of rSPI2-His<sub>6</sub> protein was done as described previously [26, 27]. Four days after induction of rSPI2-His<sub>6</sub> expression, the culture medium was collected by centrifugation. rSPI2-His<sub>6</sub> was purified, from the culture medium, on Ni-NTA-agarose with >95% purity following the procedure described by Kłudkiewicz *et al.* [27]. The culture medium without expressed protein

(*Pichia* cells transformed with the pPICZ $\alpha$ B plasmid) was used as a control medium. The recombinant SPI2 protein without histidine-tag (rSPI2) was obtained according to the procedure described previously [26,27].

#### 2.4. Fabrication of gold nanorods (GNR)

Gold nanorods were fabricated according to a reported procedure [28]. For gold-seed production, 0.5 mL of 0.01 M HAuCl<sub>4</sub> trihydrate solution in water and 0.5 mL of 0.01 M sodium citrate solution in water were added to 18 mL of deionized water and stirred. Next, 0.5 mL of freshly prepared 0.1 M NaBH<sub>4</sub> was added and the solution color changed from colorless to orange. Stirring was stopped and the solution was left undisturbed for 2 hours. The resulting spherical nanoparticles were used as gold seed. For gold nanorod growth from the seeds, three flasks were labeled A, B and C. Growth solutions A and B consisted of 9 mL of 0.1 M cetyltrimethylammonium bromide (CTAB) in water, 0.25 mL of 0.01 M HAuCl<sub>4</sub> trihydrate in water, 50  $\mu$ L of 0.1 M ascorbic acid. Growth solution C consisted of 90 mL 0.1 M CTAB, 2.5 mL 0.01 M HAuCl<sub>4</sub>, 0.5 mL 0.1 M ascorbic acid. The seed solution was added to growth solution A and shaken for 3 seconds. Then it was poured into solution B, shaken for 4 seconds and added to solution C. The mixture turned reddish in several minutes and was left overnight at room temperature. Excess CTAB was removed by centrifugation (Eppendorf MiniSpin, 1,000 rpm 5 min). Supernatant was removed and the pellet resuspended in water and stored in +4 °C.

#### 2.5. Characterization of gold nanorods (GNR) with UV-Vis and Atomic Force Microscopy (AFM)

The suspension of gold nanorods obtained according to the procedure described in Paragraph 2.4 was characterized using UV-Vis spectrophotometry and Atomic Force Microscopy Quesant-Scope Universal Scanning (Ambios Technology, USA). Scans were performed in intermittent contact, broadband wavemode using NSC16 (W<sub>2</sub>C, Si<sub>3</sub>N<sub>4</sub>) tips oscillating at base frequency of 170 kHz. Tip curvature radius was about 10 nm. Dimensions of scanned objects were measured using Quesant software delivered with the microscope.

#### 2.6. Preparation of immunosensor

Gold electrodes were cleaned in alumina with 0.3  $\mu$ m and 0.05  $\mu$ m particle diameter size, 5 minutes each). The alumina suspensions were spotted on the BAS microcloth polishing pad and gold electrodes were gently polished by doing small circles in the one direction during 5 minutes. Afterwards they were carefully rinsed and sonicated in Milli-Q water for 30 seconds. Electrochemical cleaning electrode setup: Au—working, Pt—counter, Ag/AgCl—reference. Conditions: 0.5 M H<sub>2</sub>SO<sub>4</sub> water solution, minimum potential—0.3 V, maximum potential 1.5 V, scan rate 100 mV/s, number of cycles: 3, 20 and 5. Clean gold electrodes were rinsed with ethanol and put in 10 mM 1,6-HDT in ethanol solution for 18 hours at room temperature. Test tubes containing electrodes and 1,6-HDT solution were sealed with Teflon tape and Parafilm to avoid solvent evaporation. Subsequently electrodes were rinsed with ethanol and water respectively. Next, electrodes were put in test tubes

upside down and a 10  $\mu\text{L}$  droplet of gold nanorods (GNR) suspension obtained using the procedure described in paragraph 2.4. was spotted on each gold surface. The test tubes were sealed with Parafilm and put in  $+4\text{ }^\circ\text{C}$  for 18 hours. Next, electrodes were rinsed with water and PBS pH 7.4 (137 mM NaCl, 10 mM phosphate, 2.7 mM KCl). Next, 10  $\mu\text{L}$  droplets of F(ab') solution (0.3  $\mu\text{g}/\mu\text{L}$ ) were put on the surface of each electrode and kept in  $+4\text{ }^\circ\text{C}$  for 20 hours in sealed test tubes. After incubation, electrodes were carefully rinsed with PBS. BSA solution (in 0.1 M PBS pH 7.4) in concentration of 0.5% (m/v) was used for blocking of unspecific binding sites. A 10  $\mu\text{L}$  droplet was spotted on each electrode and incubated for 2 hours. Finally, electrodes were rinsed with PBS. Fully modified electrodes were stored in refrigerator ( $+4\text{ }^\circ\text{C}$ ) in PBS buffer until use.

### 2.7. Electrochemical impedance spectroscopy (EIS) and cyclic voltammetry (CV) measurements

EIS and CV measurements were performed using Autolab potentiostat-galvanostat (Eco Chemie, The Netherlands). Electrochemical cell setup: Au (BAS, USA) as the working electrode, Ag/AgCl as reference electrode, Pt as counter electrode. Measurements were performed in solution comprised of 0.1 M PBS pH 7.4 and  $\text{K}_3[\text{Fe}(\text{CN})_6]/\text{K}_4[\text{Fe}(\text{CN})_6]$  (0.5 mM each). EIS setup: frequency range 10 kHz to 100 mHz, formal potential 0.170 V. Electron transfer resistance ( $R_i$ ) was calculated from spectra fitted by Autolab software and electrode responses were expressed as:  $(R_i - R_0)/R_0$  where  $R_i$  is the electron transfer resistance measured in the presence of the analyte and  $R_0$  the electron transfer resistance without the analyte. The amount of sample used was 10  $\mu\text{L}$  (a drop spotted on gold electrode surface). Incubation time at room temperature was 20 minutes in a sealed test tube. After applying the sample, the electrodes were conditioned in 0.1 M PBS pH 7.4 for 5 minutes. Concentrations of sample solutions of rSPI2-His<sub>6</sub> protein were as follows: 10 pg/mL (0.13 pM), 30 pg/mL (0.39 pM), 100 pg/mL (1.31 pM), 300 pg/mL (3.93 pM) and 1 ng/mL (13.10 pM). The concentrations of rSPI2 were as follow: 10 pg/mL (0.15 pM), 30 pg/mL (0.44 pM), 100 pg/mL (1.47 pM), 300 pg/mL (4.41 pM) and 1 ng/mL (14.70 pM). After the EIS assay the electrodes were put in 0.2 M Gly-HCl pH 2.8 buffer  $3 \times 2$  min and rinsed with 0.1 M PBS pH 7.4. Regenerated electrodes were used for further EIS assays until reaching 10th cycle, after which they were cleaned and fresh modification was applied.

### 2.8. Surface Plasmon Resonance (SPR)

An Autolab SPRINGLE ver. 4.2. system from Eco Chemie B. V. (The Netherlands) apparatus was used. SPR gold discs were cleaned in piranha solution ( $\text{H}_2\text{SO}_4$  96% and  $\text{H}_2\text{O}_2$  30% 7:3)  $3 \times 1$  min and thoroughly washed in Milli-Q water. After rinsing with ethanol, gold discs were put in 10 mM 1,6-HDT in ethanol for 18 hours at room temperature. Next, discs were rinsed with ethanol and water, and were covered with 50  $\mu\text{L}$  gold nanorods solution for 18 hours at  $+4\text{ }^\circ\text{C}$ . Next, 50  $\mu\text{L}$  of F(ab') solution (0.3  $\mu\text{g}/\mu\text{L}$ ) were put on the disc surface and kept in  $+4\text{ }^\circ\text{C}$  for 20 hours in sealed glass containers. After incubation, discs were carefully rinsed with PBS. Next, F(ab') modified gold discs were put in 5 mL of 0.05% BSA solution at  $+4\text{ }^\circ\text{C}$  for 2 hours. Finally the discs were rinsed and put in PBS buffer for storing between experiments.

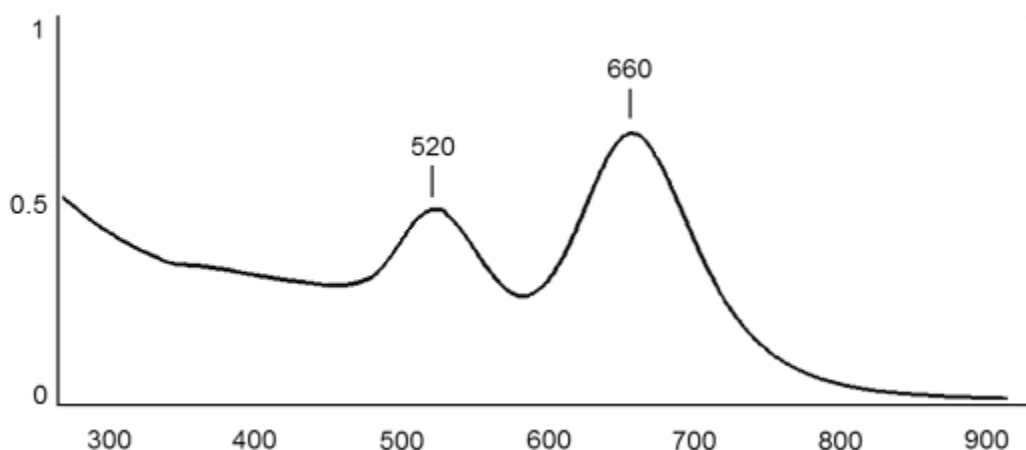
Upon obtaining a stable reading (angle shift not greater than 0.1 milidegrees per minute) in PBS buffer, 50  $\mu\text{L}$  of the first sample solution of analyte, rSPI2-His<sub>6</sub> or rSPI2, was placed on the F(ab') modified gold disc. After 20 minutes the sample solution was rinsed off with PBS buffer. The stable value of angle shift was recorded after 200 s. Samples of rSPI2-His<sub>6</sub> in concentrations 10  $\mu\text{g/mL}$  (0.13 pM), 30  $\mu\text{g/mL}$  (0.39 pM), 100  $\mu\text{g/mL}$  (1.31 pM), 300  $\mu\text{g/mL}$  (3.93 pM) and 1  $\text{ng/mL}$  (13.10 pM) were used. The concentrations of rSPI2 were as follow: 10  $\mu\text{g/mL}$  (0.15 pM), 30  $\mu\text{g/mL}$  (0.44 pM), 100  $\mu\text{g/mL}$  (1.47 pM), 300  $\mu\text{g/mL}$  (4.41 pM) and 1  $\text{ng/mL}$  (14.70 pM). After the SPR assay the modified gold discs were put in 0.2 M Gly-HCl pH 2.8 buffer  $3 \times 2$  min and rinsed with 0.1 M PBS pH 7.4. The regenerated gold discs were used for further SPR assays until reaching 10th cycle, after which they were cleaned and fresh modification was applied.

### 3. Results and Discussion

#### 3.1. Characterization of gold nanorods (GNR)

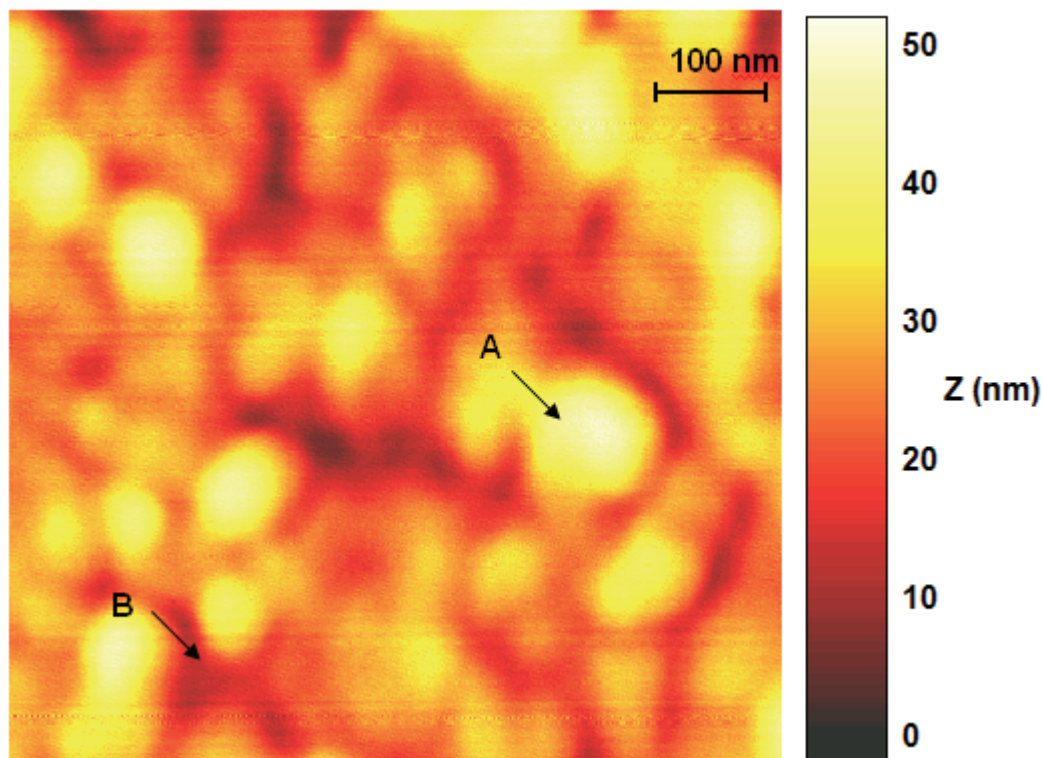
A typical UV-Vis spectrum of GNR suspension is shown in Figure 1. Absorption peaks at 520 nm and 660 nm correspond to the transverse and longitudinal plasmon bands, respectively. The positions of the peaks are influenced by the nanoparticle aspect ratio. Research done by Toderas *et al.* [29] confirm that such spectrum can be obtained for nanorods of reported size and aspect ratio.

**Figure 1.** The typical UV-Vis spectrum of GNR suspension obtained according to procedure described in Paragraph 2.4.



A typical nanorod AFM image is shown in Figure 2. The nanorods are perpendicular to the hexane-dithiol SAM. It is clearly visible that GNRs create well ordered layers with a surface larger than the Au support and more suitable for immobilization of antibodies. Results obtained using AFM show that nanorods used in this study were 70 to 90 nm wide ( $W = 80$  nm,  $SD = 14$  nm,  $n = 50$ ). This dimension can be measured on a formed nanorod layer, being the only visible full dimension. The UV-Vis spectrum of GNR (Figure 1) confirmed the aspect ratio of 2.5 [29]. This means the average nanorod in our study was 80 nm wide and 200 nm long.

**Figure 2.** AFM image of gold nanorods layer formed on 1,6-HDT modified gold plate. A—protruding nanorod, B—cracks between nanorods.



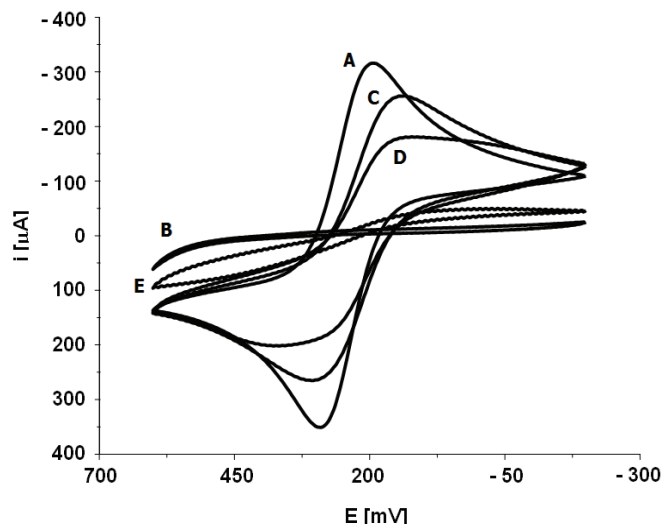
The use of nanorods as an underlayer for electrochemical biosensors is justified by their properties. Layers formed by gold nanorods are highly ordered, with nanorods protruding in one direction. This might help prevent local inconsistencies of the layer that may influence repeatability of the layer formation. In addition the deposition of GNR on the Au support increases the electrochemically available surface in comparison to bare gold or even gold nanospheres (Figure 2).

### 3.2. Characterization of the electrochemical immunosensor

The process of immunosensor fabrication is shown in Scheme S1 (Supporting Information). F(ab') fragments of immunoglobulins, which were used in the present study, are proteins with molecular mass of ca. 48 kDa. They were obtained by antibody digestion with low concentration of papain [15,16] (Scheme S2, Figure S1, Supporting Information).

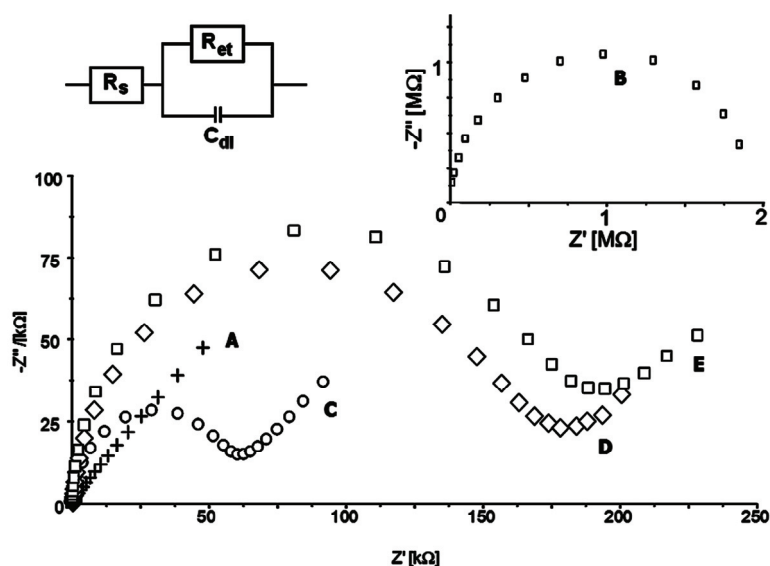
All modification steps were controlled using CV (Figure 3) and EIS (Figure 4) in the presence of 1 mM  $K_3Fe(CN)_6/K_4Fe(CN)_6$  (1:1) as redox marker. Bare gold electrodes have no obstacles affecting electron transfer which results in peak separation  $66 \pm 2$  mV. EIS control of this step produces an almost straight line as Nyquist plot ( $R_{et} = 100 \pm 10$  k $\Omega$ ). This indicates a diffusion controlled electrochemical process, not limited by electron transfer.

**Figure 3.** Cyclic voltammograms of (A) clean gold electrode surface; (B) 1,6-hexanedithiol/Au electrode; (C) gold nanorods/1,6-hexanedithiol/Au electrode; (D) F(ab')/gold nanorods/1,6-hexanedithiol/Au electrode; (E) bovine serum albumin/F(ab')/gold nanorods/1,6-hexanedithiol/Au electrode.



Electrochemical cell setup: Au (BAS, USA) as the working electrode, Ag/AgCl as reference electrode, Pt as counter electrode. Solution composition: of 0.1 M PBS pH 7.4 and  $K_3[Fe(CN)_6]$ / $K_4[Fe(CN)_6]$  (0.5 mM each).

**Figure 4.** Impedance spectra of (A) clean gold electrode surface; (B) 1,6-hexanedithiol/Au electrode; (C) gold nanorods/1,6-hexanedithiol/Au electrode; (D) F(ab')/gold nanorods/1,6-hexanedithiol/Au electrode; (E) bovine serum albumin/F(ab')/gold nanorods/1,6-hexane-dithiol/Au electrode.



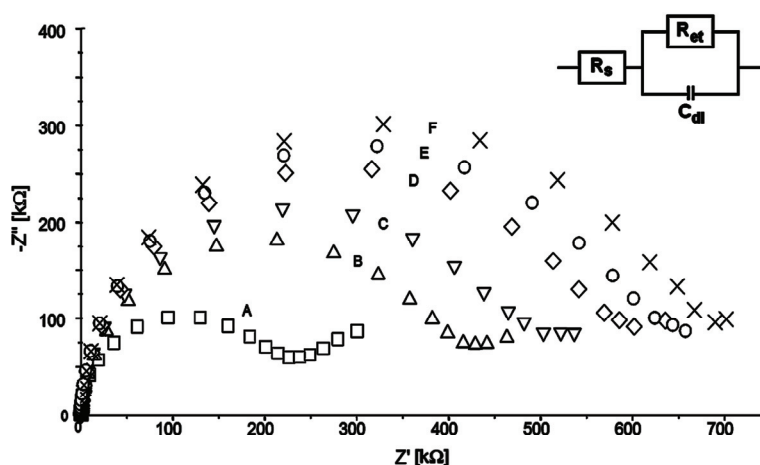
Circuit model used for fitting Nyquist plots in inset.  $R_s$ —solution resistance,  $R_{et}$ —electron transfer resistance,  $C_{dl}$ —double layer capacitance. Electrochemical cell setup: Au (BAS, USA) as the working electrode, Ag/AgCl as reference electrode, Pt as counter electrode. EIS setup: frequency range 10 kHz to 100 mHz, formal potential 0.170 V. Solution composition: of 0.1 M PBS pH 7.4 and  $K_3[Fe(CN)_6]$ / $K_4[Fe(CN)_6]$  (0.5 mM each).

The first modification step includes coating the gold layer with 1,6-hexanedithiol forming a self-assembled monolayer. This results in blocking the surface for the redox marker and can be seen in a cyclic voltammogram with no apparent peaks. Nyquist plots obtained by EIS measurements show a large semicircle at higher frequencies indicating an electron transfer limited electrode process. This increase the electron transfer resistance significantly ( $R_{et} = 730 \pm 30 \text{ k}\Omega$ ). Next the gold nanorods layer is formed to provide a conductive flexible underlayer for biomolecules [26,30-32]. The immobilization of gold nanorods (GNR) on the 1,6-hexanedithiol SAM decrease electron transfer resistance. The redox peaks separation in the range  $82 \pm 3 \text{ mV}$  were observed. EIS control of this step confirmed this phenomenon. For gold GNR layer deposited onto 1,6-hexanedithiol SAM electron transfer resistances  $R_{et} = 180 \pm 15 \text{ k}\Omega$  were recorded. F(ab') fragments were bound covalently to the GNR layer through Au-S covalent bond. This provides both the right orientation of the receptors as well as strong binding to the supporting layer [17-22,33]. F(ab') fragments create the insulating layer on the electrode surface. This results in an increase of the CV peak separation to  $130 \pm 5 \text{ mV}$  and an increase of the electron transfer resistance in EIS ( $R_{et} = 320 \pm 22 \text{ k}\Omega$ ). Blocking remaining sites of gold nanorods layer with BSA almost totally closed the electrode for the redox marker. Calculated  $R_{et}$  increased to  $650 \pm 25 \text{ k}\Omega$ .

### 3.3. Determination of the rSPI2-His<sub>6</sub> protein by EIS measurements

A typical response of the immunosensor measured by EIS is shown in Figure 5. Electron transfer resistance measured for the immunosensor in pure PBS buffer  $R_0$  (Figure 5. curve A) is used to calculate relative response towards a specific analyte. Addition of the specific antigen increases the electron transfer resistance  $R_i$  (Figure 5. curves B-F).

**Figure 5.** Impedance spectra of immunosensor: in pure PBS (A); in the presence of antigen protein rSPI2-His<sub>6</sub> in concentrations 10 pg/mL (0.13 pM) (B); 30 pg/mL (0.39 pM) (C); 0.1 ng/mL (1.31 pM) (D); 0.3 ng/mL (3.93 pM) (E) 1.0 ng/mL (13.10 pM) (F).



Electrochemical cell setup: modified Au (BAS, USA) as the working electrode, Ag/AgCl as reference electrode, Pt as counter electrode. EIS setup: frequency range 10 kHz to 100 mHz, formal potential 0.170 V. Solution composition: of 0.1 M PBS pH 7.4 and  $\text{K}_3[\text{Fe}(\text{CN})_6]/\text{K}_4[\text{Fe}(\text{CN})_6]$  (0.5 mM each). Circuit model used for fitting Nyquist plots in inset.  $R_s$ —solution resistance,  $R_{et}$ —electron transfer resistance,  $C_{dl}$ —double layer capacitance.

Electrochemical impedance measurements are characterized by relatively short assay times (4 minutes per concentration). Results obtained were well reproducible (standard deviations from nine repetitions did not exceed 8% of response values). The classic gold electrodes could be replaced with micro size electrodes. This makes EIS technique a potential candidate for development of miniaturized sensors. The proposed immunosensor was very selective and sensitive. Table 1 shows comparison of results obtained in the presence of His-tagged antigen and those obtained in the presence of antigen without his-tag. The values in Table 1 are linear equation coefficients obtained by putting concentration on logarithmic X axis and average calculated analytical response on Y axis. The first equation in Table 1 corresponds to an array of concentrations of the specific antigen (rSPI2-His<sub>6</sub>) in pure buffer. This assay, as expected, yielded the highest sensitivity and repeatability. It was performed to characterize the sensor in optimal conditions. The second equation corresponds to the negative control (rSPI2 protein without his<sub>6</sub>-tag) in 0.1 M PBS pH 7.4 buffer. It is characterized by low slope and relatively high noise, which is expected from a negative control. Third set of data shows the performance of the immunosensor in matrix—*Pichia* culture medium. It is comparable to the positive control (rSPI2-His<sub>6</sub> in PBS) in optimal conditions. Slope at the level of 83.6% of the initial value shows that the loss of sensitivity when used in matrix is not much a concern. The last result is the response of the sensor towards the matrix alone.

**Table 1.** EIS responses of the immunosensor incorporating Anti-His IgG F(ab') fragment towards rSPI-His<sub>6</sub> in PBS buffer pH 7.4 and in the presence of *Pichia pastoris* culture medium. Control samples: protein rSPI2 in PBS and medium alone.

Analyte	Response
rSPI2-His <sub>6</sub> in PBS	$y = 9.58 \log(x) + 49.21$ $r^2 = 0.997$ , $\sigma = 1.5$
rSPI2 in PBS	$y = 0.21 \log(x) + 2.35$ $r^2 = 0.659$ , $\sigma = 1.9$
rSPI2-His <sub>6</sub> in culture medium	$y = 8.01 \log(x) + 43.24$ $r^2 = 0.998$ , $\sigma = 1.1$
Culture medium without rSPI2 or rSPI2-His <sub>6</sub>	$y = 0.87 \log(x) + 3.98$ $r^2 = 0.989$ , $\sigma = 1.2$

$y$  = EIS response  $[(R_i - R_0)/R_0]$ ;  $R_i$ —electron transfer resistance at the presence of analyte;

$R_0$ —electron transfer resistance in the absence of analyte);  $x$  = analyte concentration;

10 pg/mL < X < 1 ng/mL rSPI2-His<sub>6</sub>;  $r^2$ —correlation coefficient;  $\sigma$ —standard deviation,  $n = 9$

The immunosensor incorporating GNR and anti-His IgG F(ab') fragments allows for detecting 10 pg/mL (130 fM) of rSPI2-His<sub>6</sub> protein in PBS buffer or in *Pichia* culture medium in the same range of concentrations. The linear analytical response ranged from 10 pg/mL (130 fM) to 1 ng/mL (13.10 pM).

Reusability is very important sensor parameter. Among the buffers used for regeneration of immunosensors after performing the detection of rSPI2-His<sub>6</sub> antigen, 0.1 M glycine-HCl pH 2.8 buffer was the most efficient. Nevertheless, after regeneration ten times in 0.1 M glycine-HCl pH 2.8 buffer, the immunosensor displayed sensitivity towards rSPI2-His<sub>6</sub> protein with linear response slope of 52% the initial (compared to freshly prepared sensor) value. In the case of an immunosensor incorporating whole antibody deposited on the gold nanoparticles via electrostatic interactions, a 50% decrease of sensitivity towards rSPI2-His<sub>6</sub> protein was observed after the 4th regeneration in 0.1 M glycine-HCl

pH 2.8 buffer [26]. Thus, it was shown that the covalent immobilization of F(ab') fragments on the GNR improved the reusability of immunosensor.

**Table 2.** Regeneration of the immunosensor incorporating Anti-His IgG F(ab') fragment regenerated with 0.1 M Gly-HCl pH 2.8 buffer. Response measured by EIS towards rSPI2-His<sub>6</sub> in PBS buffer pH 7.4.

rSPI2-His <sub>6</sub> in PBS	$y = 9.58 \log(x) + 49.21$ $r^2 = 0.997$ , $\sigma = 1.5$
Response after regeneration—Cycle 1	$y = 9.54 \log(x) + 48.94$ $r^2 = 0.998$ , $\sigma = 1.5$
Cycle 2	$y = 9.50 \log(x) + 48.63$ $r^2 = 0.997$ , $\sigma = 1.8$
Cycle 3	$y = 9.48 \log(x) + 48.67$ $r^2 = 0.999$ , $\sigma = 1.6$
Cycle 4	$y = 9.36 \log(x) + 44.84$ $r^2 = 0.998$ , $\sigma = 1.9$
Cycle 5	$y = 9.21 \log(x) + 40.08$ $r^2 = 0.994$ , $\sigma = 1.3$
Cycle 6	$y = 9.03 \log(x) + 37.14$ $r^2 = 0.991$ , $\sigma = 1.5$
Cycle 7	$y = 7.76 \log(x) + 32.68$ $r^2 = 0.992$ , $\sigma = 1.7$
Cycle 8	$y = 5.49 \log(x) + 24.70$ $r^2 = 0.995$ , $\sigma = 1.2$
Cycle 9	$y = 4.38 \log(x) + 17.02$ $r^2 = 0.993$ , $\sigma = 1.7$

$y$  = EIS response ( $[(R_i - R_0)/R_0]$ ;  $R_i$ —electron transfer resistance at the presence of analyte;  $R_0$ —electron transfer resistance in the absence of analyte);  $x$  = analyte concentration;

$10 \text{ pg/mL} < X < 1 \text{ ng/mL}$  rSPI2-His<sub>6</sub>;  $r^2$ —correlation coefficient;  $\sigma$ —standard deviation,  $n = 9$

Based on the parameters such as very low detection limit, 10 pg of antigen per one mL, negligible influence of culture media, reusability, proposed immunosensor could compete with the immunosensors incorporating whole antibody and based on electrochemical impedance techniques already reported in the literature [34-37]. The main disadvantage of proposed EIS based immunosensors include problematic calibration, which is done in a relative manner. It means that the basic value of impedance can vary among individual sensors and it must be compared with the values obtained for studied samples to yield an analytical response. On the other hand SPR equipment is still relatively expensive compared to electrochemical hardware.

#### 3.4. Determination of the rSPI2-His<sub>6</sub> protein by SPR measurements

A typical immunosensor response to the specific antigen recorded using the SPR equipment is shown in Figure 6. The first plateau is the basic level of angle shift observed in pure PBS buffer. Successive plateaus correspond to increasing concentrations of the rSPI2-His<sub>6</sub> protein. Their angle shift values were used for calculations of parameters characterizing the immunosensor response and are summarized in Tables 3 and 4.

**Figure 6.** Real time response of the immunosensor measured by SPR: in PBS (A); in the presence of antigen protein rSPI2-His<sub>6</sub> in concentrations: 10 pg/mL (0.13 pM), 30 pg/mL (0.39 pM), 100 pg/mL (1.31 pM), 300 pg/mL (3.93 pM) and 1 ng/mL (13.10 pM). Solution composition: rSPI2-His<sub>6</sub> protein in PBS pH 7.4 (137 mM NaCl, 10 mM phosphate, 2.7 mM KCl).

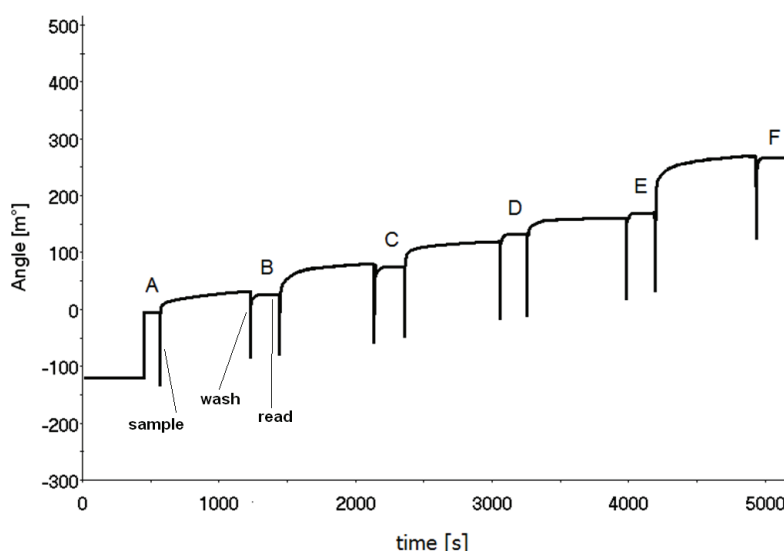


**Table 3.** SPR responses of the immunosensor incorporating Anti-His IgG F(ab') fragment towards rSPI2-His<sub>6</sub> in PBS buffer pH 7.4 (137 mM NaCl, 10 mM phosphate, 2.7 mM KCl) and in the presence of *Pichia pastoris* culture medium. The control sample: protein rSPI2 in PBS and medium alone.

Analyte	Response
rSPI2-His <sub>6</sub> in PBS	$y = 36.40 \log(x) + 183.20$ $r^2 = 0.987$ , $\sigma = 2.3$
rSPI2 in PBS	$y = 1.92 \log(x) + 13.54$ $r^2 = 0.834$ , $\sigma = 1.9$
rSPI2-His <sub>6</sub> in culture medium	$y = 32.28 \log(x) + 145.29$ $r^2 = 0.979$ , $\sigma = 2.4$
Culture medium without rSPI2 or rSPI2-His <sub>6</sub>	$y = 3.05 \log(x) + 10.74$ $r^2 = 0.963$ , $\sigma = 2.0$

$y$  = SPR response (milidegrees);  $x$  = analyte concentration;  $10 \text{ pg/mL} < X < 1 \text{ ng/mL}$  rSPI2-His<sub>6</sub>;  $r^2$ —correlation coefficient;  $\sigma$ —standard deviation,  $n=9$

Concentration range of rSPI2-His<sub>6</sub>: 10 pg/mL (0.13 pM), 30 pg/mL (0.39 pM), 100 pg/mL (1.31 pM), 300 pg/mL (3.93 pM) and 1 ng/mL (13.10 pM) and incubation time (20 min at room temperature) were analogous to those used for EIS. The calibration curve slope for the full concentration range in the case of SPR is about four times higher than in the case of EIS. Limit of detection, linear response range and capacity for regeneration are similar for both methods. Repeatability of the results for the immunosensor both in case of EIS and SPR is good. Standard deviations are relatively low (ranging from 1.1 to 2.4, see Tables 1–4). Noise to signal ratio is very good, 2% for EIS and 5% for SPR. Also the sensitivity loss when used in matrix is very satisfactory (88.7% of initial signal retained in matrix).

**Table 4.** Regeneration of the immunosensor incorporating Anti-His IgG F(ab') fragment regenerated with 0.1 M Gly-HCl pH 2.8 buffer. Response measured by SPR towards rSPI2-His<sub>6</sub> in PBS buffer pH 7.4.

rSPI2-His <sub>6</sub> in PBS	$y = 36.40 \log(x) + 183.2$ $r^2 = 0.987$ , $\sigma = 2.3$
Response after regeneration—Cycle 1	$y = 35.62 \log(x) + 176.9$ $r^2 = 0.952$ , $\sigma = 2.2$
Cycle 2	$y = 31.81 \log(x) + 153.3$ $r^2 = 0.956$ , $\sigma = 2.4$
Cycle 3	$y = 30.50 \log(x) + 146.1$ $r^2 = 0.975$ , $\sigma = 1.9$
Cycle 4	$y = 29.35 \log(x) + 140.7$ $r^2 = 0.991$ , $\sigma = 2.0$
Cycle 5	$y = 28.38 \log(x) + 137.5$ $r^2 = 0.994$ , $\sigma = 1.6$
Cycle 6	$y = 26.87 \log(x) + 125.9$ $r^2 = 0.986$ , $\sigma = 1.8$
Cycle 7	$y = 24.28 \log(x) + 118.3$ $r^2 = 0.992$ , $\sigma = 1.7$
Cycle 8	$y = 20.06 \log(x) + 112.6$ $r^2 = 0.995$ , $\sigma = 1.5$
Cycle 9	$y = 18.97 \log(x) + 104.7$ $r^2 = 0.993$ , $\sigma = 1.6$

$y$  = SPR response (milidegrees);  $x$  = analyte concentration;  $10 \text{ pg/mL} < X < 1 \text{ ng/mL}$  rSPI2-His<sub>6</sub>;  $r^2$ —correlation coefficient;  $\sigma$ —standard deviation,  $n = 9$

The measurement for full concentration range can be performed in ca. 2 hours and does not require costly labels. The SPR equipment, being more complicated and expensive than a potentiostat, is not yet suitable for miniaturized biosensors, however the sensitivity and stability of SPR measurements are impressive.

GNR proved to be an optimal underlayer for an optical sensing platform. GNR naturally enhance SPR readings because plasmons appearing on their surface are easily affected by insulators (in this case antigen proteins) adsorbed [14,38]. Regeneration results shown in Table 4 proved that reusability of the SPR immunosensor is much comparable to this of EIS immunosensor. After a week of regeneration/assay cycles formerly good sensitivity begins to drop noticeably. The several examples of SPR immunosensors incorporating F(ab') or F(ab')<sub>2</sub> fragments of antibody have been already reported [17-19,22]. Their main drawback is rather complex and multistep preparation of sensing platform and sensing element immobilization. The way of fabrication of SPR immunosensor proposed is simpler and less chemical consuming. The application of GNRs provide not only good conductive underlayer, but also allows for one step covalent immobilization of F(ab') fragment. Because of that the immunosensor proposed displayed very good analytical parameters such as low detection limit 10 pg/mL, lack of the influence of the complex medium matrix and reproducibility (standard deviations from 9 repetitions did not exceed 8% of response values).

The immunosensor incorporating F(ab') fragments covalently attached through Au-S bonds on the surfaces of gold nanoparticles showed better reusability in the comparison with one incorporating whole IgG antibody [26]. This is mainly because of different immobilization strategy. The covalent immobilization is stronger in comparison to electrostatic interactions between antibody and sensing platform. In addition, covalent bonds between Au atoms of GNPs and SH group of F(ab') fragments enabling the appropriate orientation for antigen binding [39].

#### 4. Conclusions

Immunosensor incorporating Anti-His IgG F(ab') fragment and gold nanorods for detection of his-tagged proteins is able to detect 10 pg/mL (0.13 pM) of antigen. The recognition process take place on the surface, not in the solution. Therefore, the necessary amount of F(ab') fragments is very small ( $6 \times 10^{-11}$  mols of F(ab') per electrode). It also requires no labels, which is a distinct advantage. These traits make it an easy to use and relatively cheap method of detecting antigens in complex medium. The limit of detection remains almost the same in culture medium as was observed in PBS buffer. Analytical response range for the immunosensor proposed is between 10 pg/mL (0.13 pM) and 1 ng/mL (13.1 pM) which is better in the comparison of other already reported. Immunosensor incorporating F(ab') fragments is more reusable than one incorporating whole antibody IgG.

#### Acknowledgements

This research was supported by grant Polish Ministry of Science and Higher Education No.: 2 P06T 014 29 and statutory funds of Institute of Animal Reproduction and Food Research of Polish Academy of Sciences, Olsztyn , Poland.

#### References

1. Vallina-Garcia, R.; del Mar Garcia-Suarez, M.; Fernandez-Abedul, M. T.; Mendez, F.J.; Costa-Garcia, A. Oriented immobilisation of anti-pneumolysin Fab through a histidine tag for electrochemical immunosensors. *Biosens. Bioelectron.* **2007**, *23*, 210–217.
2. Stobiecka, A.; Dvornyk, A.; Grzelak, K.; Radecka, H. Electrochemical impedance spectroscopy for the study of juvenile hormones—recombinant protein interactions. *Front. Biosci.* **2008**, *13*, 2866–2874.
3. Grzelak, K.; Kludkiewicz, B.; Kolomiets, L.I.; Dębski, J.; Dadlez, M.; Lalik, A.; Ozyhar, A. Kochman, M. Overexpression of juvenile hormone binding protein in bacteria and *Pichia pastoris*. *Protein Expr. Purif.* **2003**, *31*, 173–180.
4. Kaslow, D.C.; Shiloach, J. Production, purification and immunogenicity of a malaria transmission-blocking vaccine candidate: TBV25H expressed in yeast and purified using nickel-NTA agarose. *Biotechnology* **1994**, *12*, 494–499.
5. Kaufmann, M.; Lindner, P.; Honegger, A.; Blank, K.; Tschopp, M.; Capitani, G.; Plückthun, A.; Grütter, M.G. Crystal Structure of the Anti-His Tag Antibody 3D5 Single-chain Fragment Complexed to its Antigen. *J. Mol. Biol.* **2002**, *318*, 135–147.
6. Wu, J.; Fu, Z.; Yan, F.; Ju, H. Biomedical and clinical applications of immunoassays and immunosensors for tumor markers. *Trends Analyt. Chem.* **2007**, *26*, 679–688.
7. Guo, S.; Dong, S. Biomolecule-nanoparticle hybrids for electrochemical biosensors. *Trends Analyt. Chem.* **2009**, *28*, 96–109.
8. Tang, D.Q.; Zhang, D.J.; Tang, D.Y.; Ai, H. Amplification of the antigen-antibody interaction from quartz crystal microbalance immunosensors via back-filling immobilization of nanogold on biorecognition surface. *J. Immunol. Meth.* **2006**, *316*, 144–152.

9. Kachler, K.; Kauffmann, J.M.; Wang, J.; Svancara, I.; Vytras, K.; Neuhold, C.; Yang, Z. Sensors based on carbon paste in electrochemical analysis: A review with particular emphasis on the period 1990–1993. *Electroanalysis* **1995**, *7*, 5–22.
10. Saerens, D.; Huang, L.; Bonroy, K.; Muyltermans, S. Antibody Fragments as Probe in Biosensor Development. *Sensors* **2008**, *8*, 4669–4686.
11. Gobi, K.V.; Iwasaka, H.; Miura, N. Self-assembled PEG monolayer based SPR immunosensor for label-free detection of insulin. *Biosens. Bioelectron.* **2007**, *22*, 1382–1389.
12. Daniels, J.S.; Pourmand, N. Label-free impedance biosensors: opportunities and challenges *Electroanalysis* **2008**, *19*, 1239–1257.
13. Dudak, F.C.; Boyac, I.H. Rapid and label-free bacteria detection by surface plasmon resonance (SPR) biosensors. *Electroanalysis* **2009**, *7*, 1003–1011.
14. Pingarron, J.M.; Yanez-Sedeno, P.; Gonzalez-Cortes, A. Gold nanoparticle-based electrochemical biosensors. *Electrochim. Acta* **2008**, *53*, 5848–5866.
15. Coleman, L.; Mahler, S. Purification of Fab fragments from a monoclonal antibody papain digest by Gradiflow electrophoresis. *Protein Expr. Purif.* **2003**, *32*, 246–251.
16. Adamczyk, M.; Gebler, J.C.; Wu, J. Papain digestion of different mouse IgG subclasses as studied by electrospray mass spectrometry. *J. Immunol. Meth.* **2000**, *237*, 95–104.
17. Vikholm, I. Self-assembly of antibody fragments and polymers onto gold for immunosensing. *Sens. Actuat. B* **2005**, *106*, 311–316
18. Lee, W.; Oh, B.K.; Lee, W.H.; Choi, J.W. Immobilization of antibody fragment for immunosensor application based on surface plasmon resonance. *Colloids and Surfaces B: Biointerfaces* **2005**, *40*, 143–148.
19. Vikholm-Lundin, I.; Albers, W.M. Site-directed immobilisation of antibody fragments for detection of C-reactive protein. *Biosens. Bioelectron.* **2006**, *21*, 1141–1148.
20. Iwata, R.; Satoh, R.; Iwasaki, Y.; Akiyoshi, K. Covalent immobilization of antibody fragments on well-defined polymer brushes via site-directed method. *Colloids and Surfaces B: Biointerfaces* **2008**, *62*, 288–298.
21. Wang, H.; Wu, J.; Li, J.; Ding, Y.; Shen, G.; Yu, R. Nanogold particle-enhanced oriented adsorption of antibody fragments for immunosensing platforms. *Biosens. Bioelectron.* **2005**, *20*, 2210–2217.
22. Bonroy, K.; Frederix, F.; Reekmans, G.; Dewolf, E.; De Palma, R.; Borghs, G.; Declerck, P.; Goddeeris, B. Comparison of random and oriented immobilisation of antibody fragments on mixed self-assembled monolayers. *J. Immunol. Meth.* **2006**, *312*, 167–181.
23. Eum, N.S.; Yeom, S.H.; Kwon, D.H.; Kim, H.R.; Kang, S.W. Enhancement of sensitivity using gold nanorods- Antibody conjugator for detection of *E.coli* O157:H7. *Sens. Actuat. B* **2010**, *143*, 784–788.
24. Sudeep, P.K.; Shibu, S.T.J.; Thomas, K.G. Selective detection of cysteine and glutathione using gold nanorods. *J. Am. Chem. Soc.* **2005**, *127*, 6516–6517.
25. Shibu, S.T.J.; Ipe, B.I.; Pramod, P.; Thomas, G. Gold nanorods to nanochains: Mechanistic investigations on their longitudinal assembly using  $\alpha$ ,  $\omega$  -alkenedithiols and interplasmon coupling. *J. Phys. Chem. B.* **2006**, *110*, 150–157.

26. Wąsowicz, M.; Subramanian, V.; Dvornyk, A.; Grzelak, K.; Kłudkiewicz, B.; Radecka, H. Comparison of electrochemical immunosensors based on gold nano materials and immunoblot techniques for detection of histidine-tagged proteins in culture medium. *Biosens. Bioelectron.* **2008**, *24*, 284–289.
27. Kłudkiewicz, B.; Kodrík, D.; Grzelak, K.; Nirmala, X.; Sehnal, F. Structurally unique recombinant Kazal-type proteinase inhibitor retains activity when terminally extended and glycosylated. *Protein Expr. Purif.* **2005**, *43*, 94–102.
28. Bushbee, B.; Obare, S.; Murphy, C. An improved synthesis of high-aspect-ratio gold nanorods. *Adv. Mater.* **2003**, *15*, 414–416.
29. Toderas, F.; Iosin, M.; Astilean, S. Luminescence properties of gold nanorods. *Nuclear Instrum. Meth. Phys. Res. B* **2009**, *267*, 400–402.
30. Sharina, A.H.; Lee, Y.H.; Musa, A. Effects of Gold Nanoparticles on the Response of Phenol Biosensor Containing Photocurable Membrane with Tyrosinase. *Sensors* **2008**, *8*, 6407–6416.
31. Szymańska, I.; Radecka, H.; Radecki, J.; Kaliszan, R. Electrochemical Impedance Spectroscopy for Study of Amyloid  $\beta$ -Peptide Interactions with (-) Nicotine Ditartrate and (-) Cotinine. *Biosens. Bioelectron.* **2007**, *22*, 1955–1960.
32. Grabowska, I.; Radecka, H.; Burza, A.; Radecki, J.; Kaliszan, M.; Kaliszan, R. Association constants of pyridine and piperidine alkaloids to amyloid beta-peptide determined by electrochemical impedance spectroscopy. *Curr. Alzheimer Res.* **2010**, *7*, 165–172.
33. Esseghaier, C.; Helali, S.; Fredj, H.B.; Tlili, A.; Abdelghani, A. Polypyrrole-neutravidin layer for impedimetric biosensor. *Sens. Actuat. B* **2008**, *131*, 584–589.
34. Chen, H.; Jiang, J.H.; Huang, Y.; Deng, T.; Li, J.S.; Shen, G.L.; Yu, R.Q. An electrochemical impedance immunosensor with signal amplification based on Au-colloid labeled antibody complex. *Sens. Actuat. B* **2006**, *117*, 211–218.
35. Darain, F.; Ban, C.; Shim, Y.B. Development of a new and simple method for the detection of histidine-tagged proteins. *Biosens. Bioelectron.* **2004**, *20*, 857–863.
36. Yun, Y.H.; Bhattacharya, A.; Watts, N.B.; Schulz, M.J. A Label-Free Electronic Biosensor for Detection of Bone Turnover Markers. *Sensors* **2009**, *9*, 7957–7969.
37. Pejčić, B.; De Marco, R. Impedance spectroscopy: Over 35 years of electrochemical sensor optimization. *Electrochim. Acta* **2006**, *51*, 6217–6229.
38. Ni, W.; Ambjornsson, T.; Appell, S.P.; Chen, W.J. Observing plasmonic-molecular resonance coupling on single gold nanorods. *Nano Lett.* **2010**, *10*, 77–84.
39. Brogan, K.L.; Schoenfish, M. Influence of Antibody Immobilization Strategy on Molecular Recognition Force Microscopy Measurements. *Langmuir* **2005**, *21*, 3054–3060.